

A New Analytical Approach to Improving the Aerodynamic Performance of the Gyromill Wind Turbine

Eiji Ejiri^{1,*}, Tomoya Iwadate²

¹Department of Mechanical Science and Engineering, Chiba Institute of Technology, Narashino, Japan

²Graduate School of Chiba Institute of Technology, Narashino, Japan

*corresponding author: ejiri.eiji@it-chiba.ac.jp

Abstract The aim of this study was to clarify the current aerodynamic issues regarding the gyromill wind turbine and to propose an improved design configuration. First, the effect of two major design parameters, namely, blade thickness and blade mounting angle, on efficiency was experimentally investigated. Second, a throughflow analysis was conducted by computational fluid dynamics (CFD) based on the experimental results and a guideline for better performance was obtained. The test wind turbine had two blades, the chord length of which was 124 mm. Two symmetric profiles were used as variations in the blade profile. The following results were obtained in the experiments. (1) Efficiency was improved by increasing the blade thickness. (2) The range of the tip speed ratio in terms of high efficiency became narrower with thicker blades. SCRYU/Tetra V10, a commercial CFD code employing the finite volume method, was used in the numerical analysis of unsteady two-dimensional flow. The following results were obtained by numerical analysis. (3) The overall power coefficient of the turbine runner was higher with thicker blades than with thinner blades because the negative value of the power coefficient of the individual blades was smaller for the former blades. (4) Rotational force generated by lift in the inner circumferential direction contributed greatly to the rotation of the wind turbine runner. (5) It is possible to increase the power coefficient of the turbine runner if the blade shape is modified to increase lift in the inner circumferential direction. (6) The power coefficient of the turbine runner can be increased by suppressing flow separation.

Keywords: Wind turbine, Gyromill, Blade thickness, Blade mounting angle, CFD, PIV

1 Introduction

The need for clean and renewable energy sources has been growing in recent years, driven by concerns about environmental issues, such as global warming and air pollution, and resource problems, including depletion of fossil fuels. One promising candidate for next-generation power sources is wind power. Among the various types of wind turbines, the vertical axis gyromill variety has been drawing attention as a new type for city use because it generates high torque without depending on the wind direction and is safer and quieter [1].

Relatively few studies have been conducted on this turbine, the performance of which was experimentally investigated for a turbine with 2-5 symmetrical profile blades. Results have showed that its efficiency is relatively high among various types of vertical axis wind turbines but still lower than that of the horizontal axis wind turbine, such as the propeller type. Fewer gyromill wind turbines have been manufactured and used so far compared with other types. Therefore, further improvement in efficiency is essential in order to promote their widespread use.

The aim of this study was to clarify the current aerodynamic issues regarding the gyromill wind turbine and to propose an improved design configuration. First, the effect of two major design parameters, namely, blade thickness and blade mounting angle [2][3][4], on efficiency was experimentally investigated. Second, a throughflow analysis was conducted by computational fluid dynamics (CFD) based on the experimental results and a guideline for better performance was obtained.

2 Experiments

Figure 1 shows the wind turbine runner used in this study. The wind turbine has a 330-mm outer diameter, D , and a 300-mm height, L . The runner has two blades with a chord length, C , of 123.7 mm. Two symmetric profiles, NACA0012 and NACA0030, referred to here as Turbine 1 and Turbine 2, were used as variations in the blade profile. The blade mounting angle, θ , could be set from 0° to 40° by means of two slits cut in the blades. The blades were made of expanded polypropylene (EPP) and the two stays used to hold the blades

were made of carbon fiber reinforced plastic (CFRP). Both materials helped to lighten the turbine runner weight.

The performance of the wind turbine was measured in a wind tunnel with a rectangular discharge cross section of 350 mm x 530 mm. The turbine runner was installed 390 mm in front of the discharge opening. The axis of the turbine runner was oriented horizontally for convenience's sake. The wind velocity was 4 m/s and the typical Reynolds number based on the runner peripheral velocity and the diameter was 3.3×10^4 . Turbine performance was evaluated on the basis of the tip speed ratio, λ , and power coefficient, C_p , which were calculated from the runner rotational speed and torque measured with a torquemeter. The blade mounting angle, θ , was increased from 5° in increments of 5° , and the experiment was terminated when the runner ceased to rotate.

The experimental results for Turbines 1 and 2 are shown in Figs. 2 and 3. It is seen in Fig. 2 that the power coefficient, C_p , of Turbine 1 was maximum when θ was 15° . In addition, C_p was maximum in the range of $\lambda > 1$ for $\theta = 5^\circ - 15^\circ$. A distinctive feature of the lift-type wind turbine is that the power coefficient becomes maximum in the range of $\lambda > 1$. On the other hand, C_p is maximum in the range of $\lambda < 1$ for $\theta = 20^\circ - 25^\circ$, which is a distinctive feature of the drag-type wind turbine [5]. It is concluded that the overall performance of Turbine 1 is high for $\theta = 5^\circ - 15^\circ$ because of its lift-type nature.

The performance of Turbine 2 was measured for $\theta = 5^\circ - 35^\circ$ and the maximum power coefficient was obtained at $\theta = 10^\circ$, as shown in Fig. 3. This means that the maximum efficiency of Turbine 2 is higher than that of Turbine 1. This is probably because the blades of Turbine 2 are thicker and tend not to suffer flow separation. However, the range of the tip speed ratio in terms of a high power coefficient is narrower for Turbine 2. This is also probably because the blades are thicker, which means that their rotational force decreases due to increased drag away from the peak efficiency point.

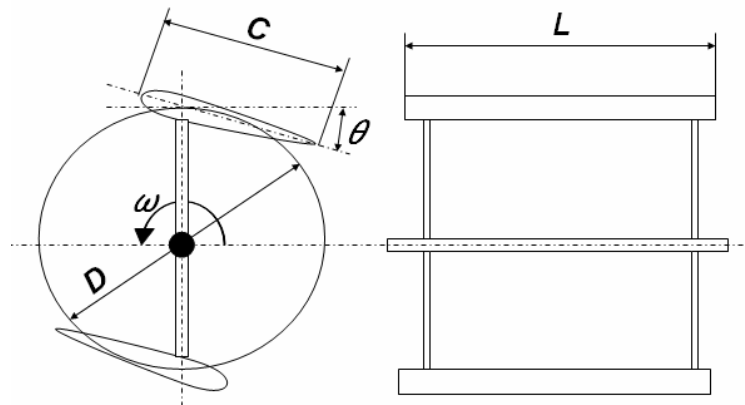


Fig. 1 Test wind turbine runner

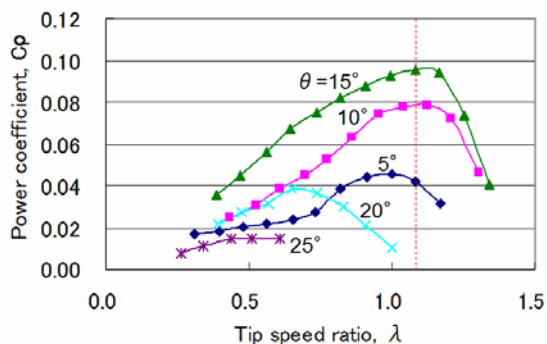


Fig. 2 Characteristic curves of Turbine 1

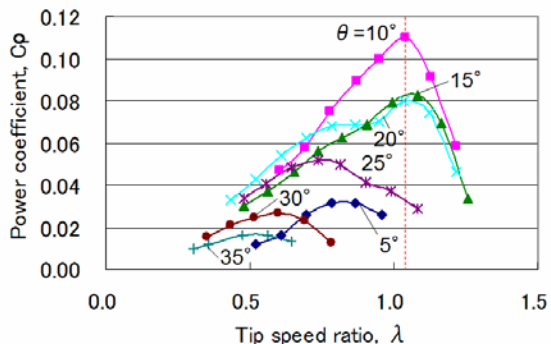


Fig. 3 Characteristic curves of Turbine 2

Flow was visualized by Particle Image Velocimetry (PIV) in order to validate the prediction accuracy of the numerical analysis. Figure 4 shows a schematic diagram of the experimental PIV setup. Pictures of tracer particles at two consecutive times were taken with a high-speed video camera synchronously with the rotation of the turbine runner. For that purpose, a picture was taken when an image sensor detected the laser light reflected on the mirror installed on the rotating disc.

The measurements were conducted at the theoretical maximum lift point [1] under the conditions of $\lambda=1.08$ and $\theta=15^\circ$ in a wind velocity of 4 m/s. The PIV visualization results are shown in Fig. 5. It can be seen that the separation region for Turbine 2 is smaller than for Turbine 1 probably because the blade thickness of the former was greater and the adverse pressure gradient after the leading edge was smaller compared with Turbine 1.

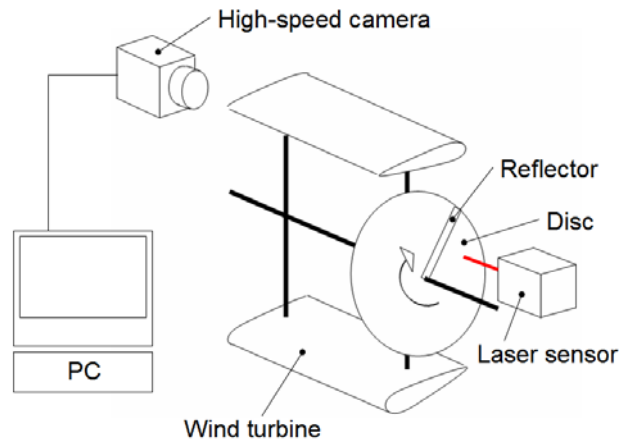


Fig. 4 PIV system synchronized with rotating blade

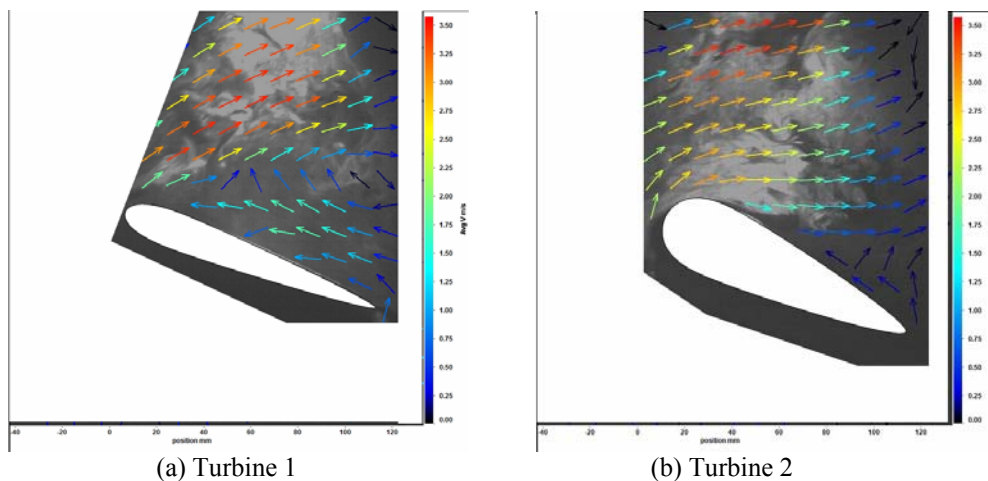


Fig. 5 Visualized velocity vectors at theoretical maximum lift point by PIV

3 Numerical Analysis

SCRYU/Tetra V10, a commercial CFD code employing the finite volume method, was used in the numerical analysis of unsteady two-dimensional flow. The governing equations were the continuity equation and the Reynolds Averaged Navier-Stokes equations. The standard $k-\epsilon$ model was used as a turbulence closure model. The total computational domain included the sufficiently upstream and downstream regions. The total number of the computational meshes was about 3.32×10^6 . The computational meshes around the turbine runner are shown in Fig. 6.

The rotational angle of the blades, α , is defined as 0° when the straight line connecting the rotation center and the lift center of the blade is perpendicular to the direction of the uniform flow. The lift center is 30.9 mm after the leading edge of the blade. α is positive in the counter-clockwise direction, as shown in Fig. 7.

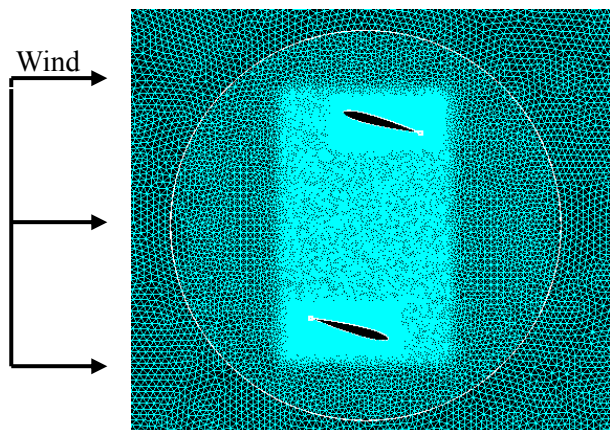


Fig. 6 Computational meshes around turbine runner

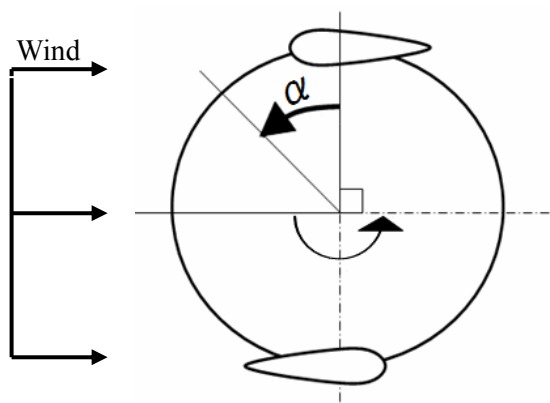


Fig. 7 Definition of angle α

The computed velocity vectors at the theoretical maximum lift point are shown in Fig. 8, which correspond to the measured ones in Fig. 5. It can be seen that the flow directions are qualitatively consistent in these figures over a wide range of flow fields. The magnitude of the velocity vectors in Fig. 5 are little bit smaller than that in Fig. 8, however, this discrepancy can be attributed to the error generated by insufficient tracer particle dispersion. These results confirm that the computational analysis is sufficiently accurate for practical use.

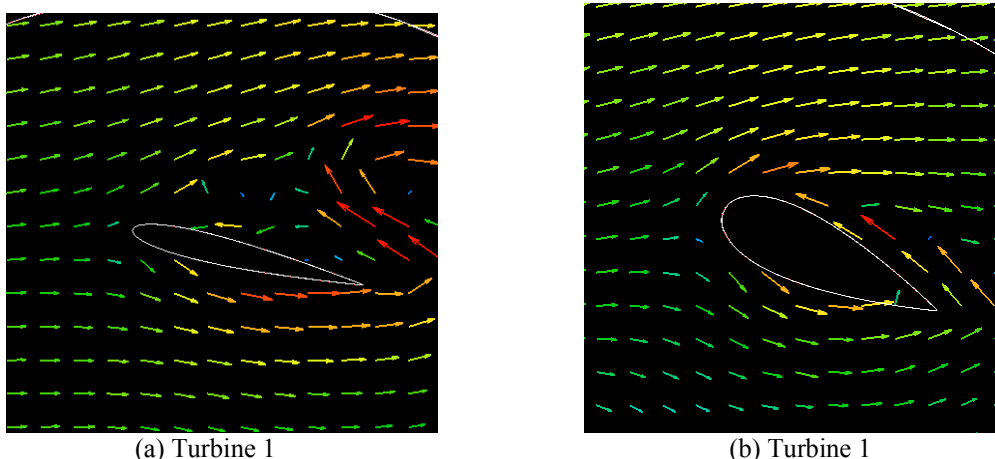


Fig. 8 Computed velocity vectors at theoretical maximum lift point

The computational results at the operating points where the highest C_p was obtained in the experiments are shown below. They correspond to $\lambda=1.08$ at $\theta=15^\circ$ for Turbine 1 and $\lambda=1.04$ at $\theta=10^\circ$ for Turbine 2. Time histories of the computed C_p for Turbines 1 and 2 are shown in Figs. 9 and 10, respectively. Time histories of the computed C_p for the individual blades (Wing 1 and Wing 2) are also shown in the figures. These figures show the change in C_p relative to α as the turbine runner rotated. For reference, the computed overall value of C_p averaged for $\alpha=0^\circ-360^\circ$ was larger than the experimental value by 14.4% for Turbine 1 and smaller by 11.2% for Turbine 2.

C_p of Wing 1 displays large negative values in a range of $\alpha=190^\circ-20^\circ$ for Turbine 1 as shown in Fig. 9. This is because the angle of attack of the blades continuously changes due to runner rotation. However, the overall C_p shows a positive value if the C_p values of the two individual blades (Wings 1 and 2) are added together. In order to improve the performance of the wind turbine, it is necessary either to decrease the negative value of C_p for one blade or to increase the positive value of C_p for one blade.

C_p of Wing 1 displays large negative values in range of $\alpha=220^\circ-30^\circ$ for Turbine 2 as shown in Fig. 10, and the range of α showing a negative value over one rotation is larger for Turbine 2 than for Turbine 1. However, the efficiency of Turbine 2 is higher than that of Turbine 1 because the negative value in C_p of Wing 1 for Turbine 2 is smaller than that for Turbine 1. The main cause of this phenomenon is a gradual peak in C_p of Wing 1 for Turbine 2 around $\alpha=300^\circ$. No such peak is seen for Turbine 1.

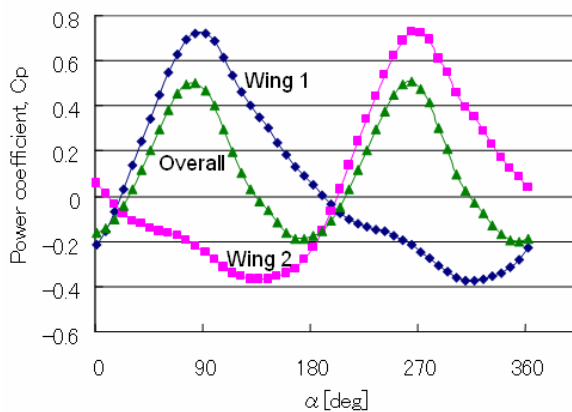


Fig. 9 Power coefficients in terms of α (Turbine 1)

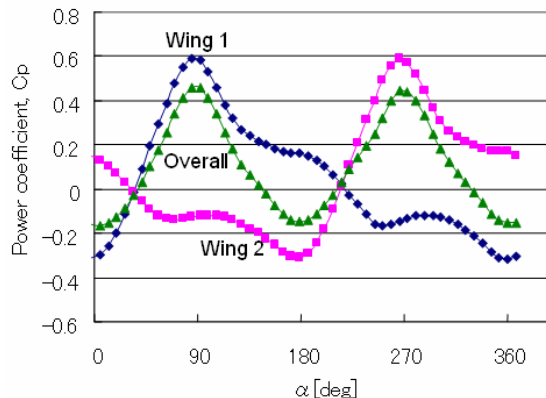


Fig. 10 Power coefficients in terms of α (Turbine 2)

Figure 11 shows the pressure distribution around Wing 1 of Turbines 1 and 2 at $\alpha=300^\circ$. It is seen that a large area of negative pressure is generated over the right-hand side of the blade in Turbine 1, which is indicated by the red oval in Fig. 11(a). This is because an abrupt change in the flow direction gives rise to separation in Turbine 1. Negative pressure is also generated in Turbine 2 and is indicated by the red oval in Fig. 11(b). However, the area is much smaller compared with Turbine 1. This is of course because a gradual change in flow direction tends to obstruct separation in Turbine 2. This is directly linked to the fact that the negative C_p value of Wing 1 for Turbine 2 is smaller than that for Turbine 1.

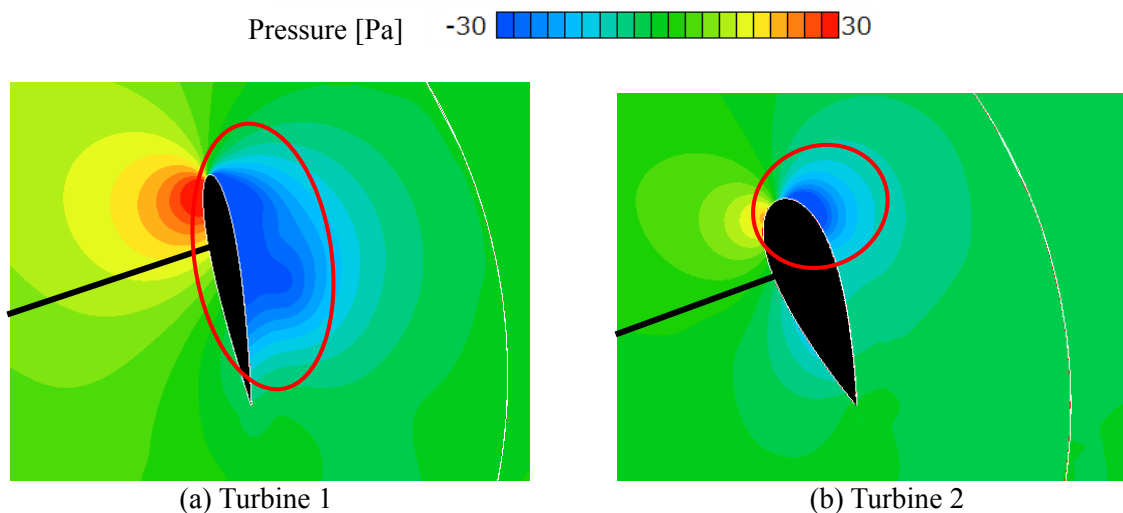


Fig. 11 Pressure distribution around Wing 1 ($\alpha=300^\circ$)

Figures 12(a) and 12(b) show the pressure distributions around Wing 1 for Turbines 1 and 2 when C_p of Wing 1 has a maximum value. In these figures it is seen that C_p is maximum when the uniform flow impinges on the outer side of the blade. No significant difference in pressure distribution is found between the two cases. The relationship between the aerodynamic forces and the blade position at this moment is shown in Fig. 13, where F is the rotational force acting on the turbine blade and A is the distance from the center of rotation of the turbine runner to the acting point of the lift. The rotational force, F , is composed of two forces, one of which is a peripheral component of the lift and the other a peripheral component of the drag acting on the blade. The wind turbine runner was assumed to generate rotational torque by the lift in the outer circumferential direction according to the literature [1]. However, it is seen in these analysis results that the lift in the inner circumferential direction significantly contributes to the rotational torque.

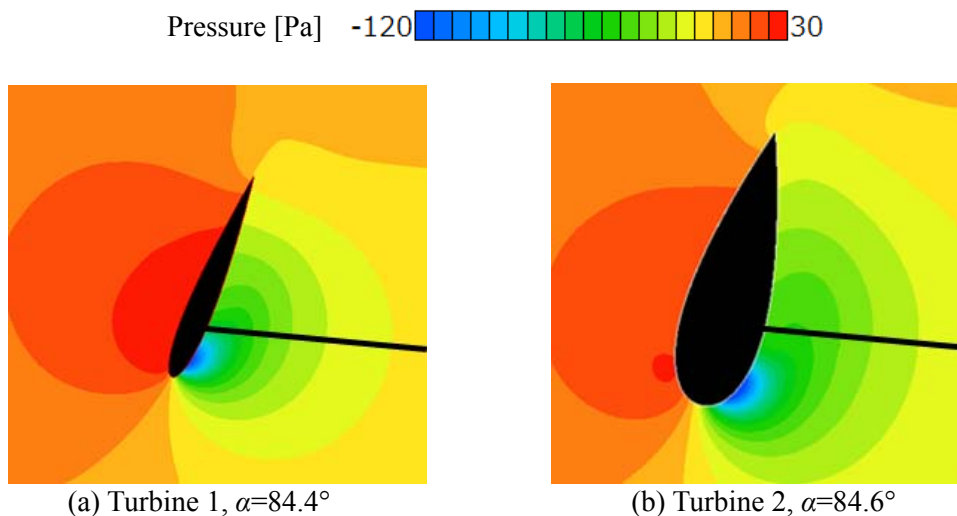


Fig. 12 Pressure distribution around Wing 1 at maximum torque

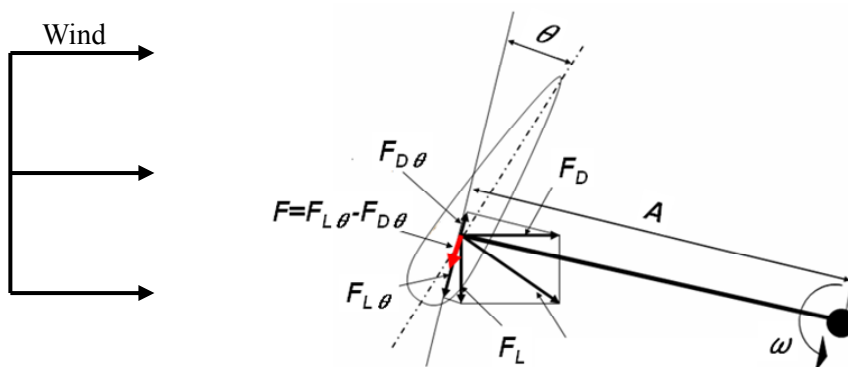


Fig. 13 Relationship between aerodynamic and rotational forces

Figure 14 shows the pressure distribution around Wing 1 for Turbines 1 and 2 when C_p of Wing 1 has a minimum value. Minimum C_p occurs at $\alpha=318^\circ$ for Turbine 1, which corresponds to Fig. 14(a), and at $\alpha=359^\circ$ for Turbine 2, which corresponds to Fig. 14(b). The difference in α is not small probably because the causes of the minimum C_p are different. In Turbine 1, on the one hand, the rotational force is reduced by negative pressure due to separation occurring at the outer peripheral portion of the blades as shown in Fig. 14(a). In Turbine 2, on the other hand, the rotational force is reduced by positive pressure near the leading edge, as indicated in the blue oval in Fig. 14(b). This phenomenon is probably caused by the blade thickness. Some countermeasures such as changing the blade shape must be taken in order to remove the positive pressure.

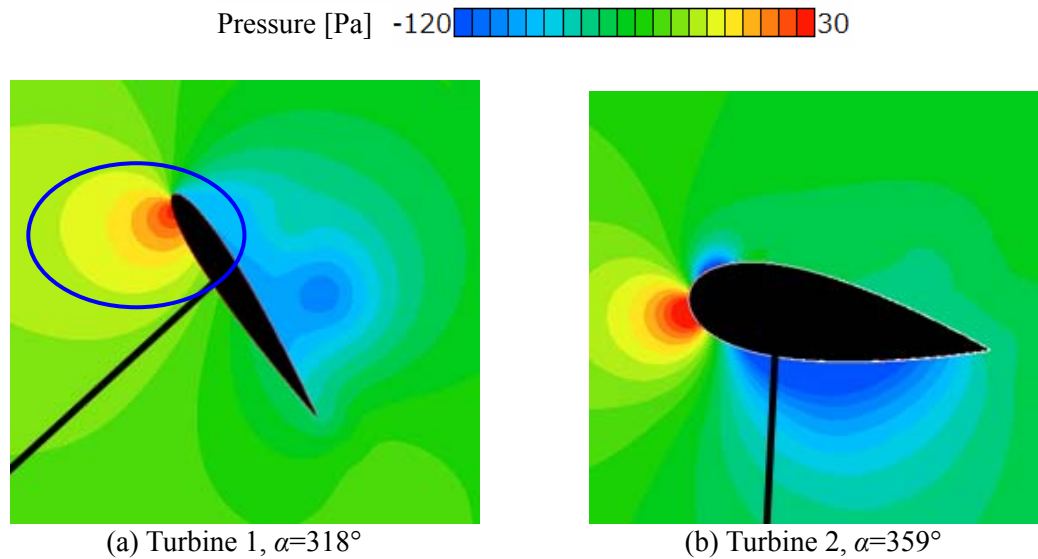


Fig. 14 Pressure distribution around Wing 1 at minimum torque

4 Conclusions

The following results were obtained in the experiments conducted on the test gyromill wind turbine.

(1) Efficiency was improved by increasing the blade thickness.

(2) The range of the tip speed ratio in terms of high efficiency became narrower with thicker blades.

The following results were obtained by numerical analysis of two-dimensional flow around the test gyromill wind turbine.

(3) The overall power coefficient of the turbine runner was higher with thicker blades than with thinner blades because the negative value of the power coefficient of the individual blades was smaller for the former blades.

(4) Rotational force generated by lift in the inner circumferential direction contributed greatly to the rotation of the wind turbine runner.

(5) It is possible to increase the power coefficient of the turbine runner if the blade shape is modified to increase lift in the inner circumferential direction.

(6) The power coefficient of the turbine runner can be increased by suppressing flow separation.

References

- [1] Matsumoto F, Ushiyama I and Nishizawa Y (2011) Guidebook for Making Vertical Axis Wind Turbine, Powersha Co., pp 13-25, (in Japanese).
- [2] Erickson D W, Wallace J J and Pinaire J (2011) Performance Characterization of Cyclic Blade Pitch Variation on a Vertical Axis Wind Turbine, American Institute of Aeronautics and Astronautics, 49th AIAA Aerospace Sciences Meeting including the New Horizons Forum and Aerospace Exposition, pp 2-14.
- [3] Inoue R, Fujimoto I, Hirano T, Hiramoto M and Ishii S (2008) A Study on the Aerodynamic Performance of Vertical Axis Wind Turbine (Effect of Rotational Speed), Gas Turbine Society of Japan, Gas Turbine Regular Conference Proceedings (36), pp 79-83, (in Japanese).
- [4] Nan K, Hirano T, Fujimoto I, Hiramoto M, and Niehuis R (2011) Experimental Survey on Unsteady Aerodynamic Characteristics, Gas Turbine Society of Japan, Gas Turbine Regular Conference Proceedings (39), pp 181-185, (in Japanese).